FERM Domain of Moesin Desorbs the Basic-Rich Cytoplasmic Domain of L-Selectin from the Anionic Membrane Surface

Wei Deng, **Sungyun Cho**, and **Renhao Li**
Aflac Cancer and Blood Disorders Center, Department of Pediatrics, Emory University School of Medicine, 2015 Uppergate Drive NE, Room 440, Atlanta, GA 30322, USA

Abstract

Moesin and calmodulin (CaM) jointly associate with the cytoplasmic domain of L-selectin in the cell to modulate the function and ectodomain shedding of L-selectin. Using fluorescence spectroscopy, we have examined the association of moesin FERM domain with the recombinant transmembrane and cytoplasmic domains of L-selectin (CLS) reconstituted in model phospholipid liposomes. The dissociation constant of moesin FERM domain to CLS in the phosphatidylcholine liposome is about 300 nM. In contrast to disrupting the CaM association with CLS, inclusion of anionic phosphatidylserine lipids in the phosphatidylcholine liposome increased the apparent binding affinity of moesin FERM domain for CLS. Using the environmentally sensitive fluorescent probe attached to the cytoplasmic domain of CLS and the nitroxide quencher attached to the lipid bilayer, we showed that the association of moesin FERM domain induced the desorption of the basic-rich cytoplasmic domain of CLS from the anionic membrane surface, which enabled subsequent association of CaM to the cytoplasmic domain of CLS. These results have elucidated the molecular basis for the moesin/L-selectin/CaM ternary complex and suggested an important role of phospholipids in modulating L-selectin function and shedding.

Keywords

ectodomain shedding; juxtamembrane region; protein-lipid interaction; moesin; l-selectin

Introduction

Protein ectodomain shedding, in which the extracellular domain of a membrane protein is cleaved by membrane-associated metalloproteinases or shed-dases, is an important step in many signaling pathways [1]. Alteration in the shedding step can lead to cardiovascular diseases, cancer and neurologic diseases [2–4]. Ectodomain shedding of many proteins is mediated by highly regulated mechanisms [5]. Involved in the regulation mechanisms are certain intracellular proteins, which interact directly with the cytoplasmic domain of either sheddases or shedding substrates and regulate the proteolysis step on the extracellular side of the membrane. The molecular mechanisms underlying the across-the-membrane regulation of ectodomain shedding remain unclear [5].

Intracellular regulation of L-selectin shedding is one of the best-characterized examples [6]. As a primary adhesion receptor mainly expressed on the leukocyte surface, L-selectin binds to carbohydrate-specific ligand and mediates recruitment of naive lymphocytes from the bloodstream to secondary lymphoid organs [7]. Treatment of naive lymphocytes with

phorbol-12-myristate-13-acetate (PMA) induces rapid shedding of surface L-selectin via a protein kinase C-dependent pathway [8–10]. As a type I transmembrane protein, L-selectin is composed of an N-terminal C-type lectin domain, an epidermal growth factor-like domain, two short consensus repeats, a stalk region containing the shedding cleavage site, a transmembrane domain and a short cytoplasmic tail (Fig. 1a). Upon leukocyte adhesion and activation, L-selectin is rapidly cleaved at the peptide bond between residues Lys283 and Ser284 in the stalk region [11]. Containing only 17 residues, the cytoplasmic domain of L-selectin participates in the regulation of L-selectin shedding, as a number of mutations in the cytoplasmic domain have been reported to impact either constitutive or PMA-induced shedding of L-selectin [8,10,12,13].

Moreover, truncation of the cytoplasmic domain or replacement of the transmembrane and cytoplasmic domains of L-selectin significantly altered the shedding level of L-selectin [14]. Intracellular proteins moesin and calmodulin (CaM) have been found to interact with the L-selectin cytoplasmic domain and suggested to regulate shedding of L-selectin [6,8,12,13].

Moesin is a founding member of the band 4.1-ezrin-radixin-moesin (FERM) protein family that shares the namesake structural domain [15,16]. As a cytoskeleton adaptor protein, moesin is located mainly in filopodia and other membranous protrusions and organizes the cortical cytoskeleton by linking filamentous actin to the plasma membrane [17]. Moesin is composed of an N-terminal FERM domain, a long α-helix linker region and a C-terminal FERM-associating domain (Fig. 1b). The self-associated N- and C-terminal domains mask the ligand-binding sites in the FERM domain and maintain moesin in a dormant or inactive state [18]. Binding of phosphatidylinositol-4,5-bisphosphate (PIP$_2$) and/or phosphorylation of Thr558 in the C-terminal domain induce the activation of moesin by dissociating its N-domain from C-domain [19–22]. Upon activation, the N-terminal FERM domain becomes available for binding to the cytoplasmic domain of a number of receptors [23–27]. In particular, moesin binds to the juxtamembrane region of the L-selectin cytoplasmic tail in PMA-stimulated but not unstimulated leukocytes [8]. Certain mutations in the cytoplasmic domain of L-selectin that disrupt the association of moesin and L-selectin have been shown to confer L-selectin the resistance to PMA-induced shedding, suggesting that moesin association facilitates shedding of L-selectin [13]. It is thought that moesin may bring L-selectin close to its sheddase through its link to cortical actin filaments [28]. In contrast to moesin, CaM was postulated to play an inhibitory role in the regulation of L-selectin shedding because treatment of CaM inhibitors up-regulated L-selectin shedding in the cell [6]. CaM interacts with isolated L-selectin cytoplasmic peptide with modest affinity and in a calcium-independent manner [6,29]. Moreover, it was recently reported that moesin and CaM can concurrently associate with the L-selectin cytoplas-mic domain [30]. However, it is not clear how moesin and CaM accomplish their respective effects on L-selectin shedding.

We have previously characterized a recombinant L-selectin fragment named CLS in phospholipid bilayers [29,31]. CLS contains both transmembrane and cytoplasmic domains of human L-selectin (Fig. 1a). It is a monomer in detergent micelles and membranes [31]. The transmembrane domain of CLS adopts an α-helical structure that traverses the membrane bilayer, and the adjacent cytoplasmic domain is enriched in basic residues and can adhere to the membrane that is enriched with anionic phospholipids [29]. Such membrane association keeps the L-selectin cytoplasmic tail from interacting with CaM, suggesting that CaM alone may not regulate L-selectin shedding [29]. Moesin can also bind PIP$_2$ and, with a weaker affinity, phosphatidyl-serine (PS) [32,33]. To understand how the membrane bilayer affects the association of L-selectin with moesin, we have characterized the association of moesin with CLS in membrane conditions. We report that, in contrast to CaM [29], moesin can bind and move the L-selectin cytoplasmic domain away from the anionic membrane surface. Such separation allows subsequent CaM association with the L-

selectin cytoplasmic domain and thus formation of the moesin/CLS/CaM ternary complex. By elucidating the effect of anionic lipids on these interactions, our finding helps us to shed light on the molecular mechanisms underlying regulation of ectodomain shedding.

Results

Association of moesin FERM domain with water-soluble ʟ-selectin cytoplasmic peptides

Two synthetic water-soluble peptides were used first in our characterization of the association between recombinant human moesin FERM domain (moesin-FERM) and the ʟ-selectin cytoplasmic domain (Fig. 1). The first peptide, named ARR18, corresponds to the cytoplasmic domain of human ʟ-selectin (residues Ala317–Tyr334). The other pep-tide, named TMR-ARR18, shares the same sequence except that the N-terminal residue is changed to cysteine, in which the thiol group is further decorated with a tetramethylrhodamine-5-maleimide (TMR) fluorophore group. Since ARR18 does not contain any tryptophan (Trp) residues, the intrinsic Trp fluorescence emission of moesin-FERM was recorded as ARR18 was added to moesin-FERM in 50 mM Tris–HCl and 150 mM NaCl (pH 7.4) and at the room temperature (Fig. 2a and b). When excited at 295 nm, moesin-FERM produced a typical Trp emission spectrum with an emission maximum at 333 nm. Addition of ARR18 induced a significant dose-dependent decrease in the Trp fluorescence emission (Fig. 2a). Titration of ARR18 to moesin-FERM, monitored by the change in Trp fluorescence, was fitted to the standard hyperbolic function, and an equilibrium dissociation constant (K_d) of 196 ± 15 nM was obtained (Fig. 2b and Table 1). It was noted that Trp fluorescence deviated from the fitted curve at high concentration of ARR18. The association between recombinant moesin in its full-length form and ARR18 was also monitored in a similar fashion. The addition of ARR18 to moesin induced little detectable change in Trp fluorescence of moesin, indicating that moesin does not associate with ARR18 (Fig. 2c and d).

The association of moesin-FERM to TMR-ARR18 was monitored by the change in the TMR fluorescence. When excited at 542 nm, TMR-ARR18 dissolved in the same buffer as above showed a TMR emission spectrum with an emission maximum at 575 nm. Addition of moesin-FERM to the TMR-ARR18 solution induced an increase in TMR fluorescence emission (Fig. 2e). Titration of moe-sin-FERM to TMR-ARR18 could be fitted to the same hyperbolic function with a K_d of 214 ± 22 nM (Fig. 2f and Table 1). In contrast, addition of moesin to TMR-ARR18 induced little change in TMR fluorescence (Fig. 2g and h). Overall, these results demonstrated that moesin-FERM but not full-length moesin interacts with the ʟ-selectin cytoplasmic domain. The similarity of K_d values obtained from ARR18 and TMR-ARR18 titration experiments indicates that conjugation of TMR to residue 317 of the ʟ-selectin cytoplasmic domain does not significantly alter the association of ARR18 with moesin-FERM.

Association of moesin FERM domain with CLS in membrane bilayers

To assess the effect of membrane bilayer on the association of moesin-FERM with the ʟ-selectin cytoplasmic domain, we next characterized the association of moesin-FERM with CLS reconstituted in the 1-palmitoyl-2-oleoyl-*sn*-glycero-3-phospho-choline (POPC) liposome (CLS/POPC), which provided a neutrally charged membrane environment. As shown in an earlier study, CLS in the POPC liposome adopts primarily an α-helical conformation, with its cytoplasmic domain exposed to the aqueous solution [29]. Unlike the measurements of the ARR18 peptide, Trp fluorescence could not be utilized here because both CLS and moesin-FERM contain Trp residues. Instead, a TMR group was conjugated to CLS at residue 317 to generate TMR-CLS(317) and the change in TMR fluorescence was followed during the titration of moesin-FERM. The labeled CLS was reconstituted in the

POPC lipo-some at the 1:1000 molar ratio [TMR-CLS(317)/POPC] and diluted in 50 mM Tris and 150 mM NaCl (pH 7.4) to a final CLS concentration of 5 nM (determination of CLS concentration is described in Materials and Methods). Moesin-FERM used for the titration experiment was dissolved in the same buffer containing 5 nM TMR-CLS(317)/POPC to keep the concentration of CLS constant (Fig. 3a). The dose-dependent change in TMR fluorescence emission induced by the addition of moesin-FERM was fitted to the hyperbolic function with a K_d of 322 ± 43 nM (Fig. 3b). Due to the closed structure of a liposome, about half of TMR-CLS(317) was embedded in the bilayer in an orientation that placed its cytoplasmic domain inside the liposome and thus unavailable for moesin-FERM association [29]. In this study, since the concentration of TMR-CLS(317) was much lower than the obtained K_d, the presence of unbound TMR-CLS(317) inside the liposome should not affect the measurement.

Compared to the association of moesin-FERM with TMR-ARR18 in aqueous solutions, the association of moesin-FERM with TMR-CLS(317)/POPC had a slightly larger K_d (Table 1). The difference is likely due to the presence of the phospholipid bilayer, which may limit to a certain extent the accessibility of the L-selectin cytoplasmic domain for ligand binding. Interestingly, the TMR fluorescence emission intensity in TMR-CLS(317)/POPC was decreased upon moesin-FERM association, in contrast to the increasing effect of moesin-FERM on the TMR fluorescence in TMR-ARR18 (Figs. 2e and 3a). TMR is an environmentally sensitive fluorophore [34,35]. An increase in its fluorescence emission typically indicates a movement of the TMR group to a more hydrophobic environment and vice versa. Thus, the increased TMR fluorescence in TMR-ARR18 indicates that, upon its association with moesin-FERM, the environment around residue 317 becomes more hydrophobic, which is consistent with the model that residue 317 becomes close to moesin-FERM upon association. Likewise, the decreased TMR fluorescence in TMR-CLS(317)/POPC indicates that, upon association with moe- sin-FERM, the TMR group attached to residue 317 is exposed to a less hydrophobic environment. However, since residue 317 is located at the junction between transmembrane and cytoplasmic domains of L-selectin (Fig. 1), it is not clear whether the moesin-FERM-induced environmental change entails a separation between residue 317 and the membrane bilayer.

Moesin-FERM association induces the desorption of L-selectin cytoplasmic domain from the negatively charged membrane surface

To explore the possibility that moesin-FERM association with CLS induces a change in the cytoplasmic domain, we used TMR-labeled CLS_S329C (TMR-CLS) [29,31] in this study henceforth. Residue 329 is located in the distal portion of the L-selectin cytoplasmic domain and outside the basic-rich juxtamembrane region (Fig. 1a). TMR-CLS reconstituted in phospholipid liposomes have been employed in earlier studies to demonstrate the association of the cytoplasmic domain of CLS with anionic membrane bilayer [29]. Here, to first demonstrate the association of TMR-CLS with moesin-FERM, TMR-CLS was reconstituted in the POPC liposome at the 1:1000 molar ratio (TMR-CLS/POPC) and diluted in 50 mM Tris and 150 mM NaCl (pH 7.4) buffer. Like TMR-CLS(317)/POPC, titration of moesin-FERM caused a decrease in the TMR fluorescence (Fig. 3c and d). The K_d fitted to the titration curve was 302 ± 48 nM, indistinguishable from that obtained for TMR-CLS(317)/POPC association with moesin-FERM (Table 1). Thus, the conjugation of TMR to residue 329 does not alter significantly the interaction of moesin-FERM with CLS. Moreover, it is noteworthy that the steady-state TMR fluorescence intensity of TMR-CLS/POPC is markedly lower than that of TMR-CLS(317)/POPC. This is consistent with the difference in membrane proximity between residues 317 and 329 in POPC liposomes.

To characterize the association of moesin-FERM with TMR-CLS in an environment that mimics the anionic inner leaflet of the plasma membrane, we reconstituted TMR-CLS into liposomes composed of POPC and 1-palmitoyl-2-oleoyl-*sn*-glycero-3-phospho-L-serine (POPS) in various ratios. The average content of PS lipids in the leukocyte cell membrane is roughly 7.5% [36]. Considering the asymmetric distribution of PS in the cell membrane, the actual content of PS in the inner leaflet of the plasma membrane may be close to 15%. Thus in this study, the POPS content in the POPC/POPS liposome was varied from 5% to 20% to mimic the cell membrane. As shown in Fig. 4a, the TMR-CLS fluorescence increases with the percentage of POPS in the liposome. Such increase is not due to the variation in TMR-CLS concentration among the CLS liposome samples because all samples produced the same TMR fluorescence emission spectra after 10% SDS was added to dissolve all the liposomes (Fig. 4b). Thus, the increase in TMR fluorescence reflects the change in the environment around the TMR group. It indicates that the liposome with higher PS content provides a more hydrophobic environment for the TMR group, which is consistent with the earlier finding that the cytoplasmic domain of CLS associates with the anionic membrane surface [29].

Addition of moesin-FERM reduced the intensity of TMR fluorescence, and the extent of reduction was the largest in the liposome with the highest POPS content (Fig. 4c). Each titration curve was fitted to the simple hyperbolic equation to obtain apparent dissociation constants that ranged from 133 ± 35 nM in 5% POPS liposomes to 70 ± 9 nM in 20% POPS liposomes (Table 1). The increased affinity of moesin-FERM for TMR-CLS in POPS-containing liposomes is consistent with earlier reports that moesin-FERM can interact with anionic membrane surface [20,32,33,37]. Importantly, the TMR fluorescence at the saturating concentration of moesin-FERM was largely the same for all TMR-CLS liposomes, regardless of the lipid composition in each liposome (Fig. 4c), indicating that the environment around the TMR group in the moesin-FERM/CLS complex is not influenced by the lipid composition of the liposome. Overall, these results suggest that the TMR group, and by extension residue 329 and surrounding residues, is separated from the membrane surface upon association of moesin-FERM.

To test by another method whether moesin-FERM desorbs the cytoplasmic domain of CLS from the PS membrane surface, we reconstituted TMR-CLS in the POPC liposome that contained 10% 1-palmitoyl-2-stearoyl-(5-doxyl)-*sn*-glycero-3-phosphocholine (DoxylPC) in addition to 15% POPS and compared it to TMR-CLS in the 85% POPC/15% POPS liposome at the same peptide concentration and the same 1:1000 peptide-to-lipid molar ratio (Fig. 5a and b). The nitroxide group at the C5 position in DoxylPC is located in the hydrophobic portion of the membrane bilayer but close to the hydrophilic surface. Its ability to quench a nearby fluorophore has been utilized to probe the molecular interactions in lipid bilayers [38–40]. Since the cytoplasmic domain of CLS associates with the PS-containing membrane, it is not surprising that the TMR-CLS fluorescence emission in the 75% POPC/10% DoxylPC/15% POPS lipo-some was significantly lower than that in the 85% POPC/15% POPS liposome (Fig. 5a). More importantly, addition of moesin-FERM to TMR-CLS in the DoxylPC-containing liposome induced an increase in TMR fluorescence and, therefore, an increase in distance between DoxylPC and TMR (Fig. 5c). The titration curve was fitted with an apparent K_d of 96 ± 18 nM (Fig. 5d and Table 1), comparable to those obtained in DoxylPC-free liposomes, which indicated that the association of moesin-FERM with TMR-CLS was not affected by the presence of DoxylPC. Overall, these results provide additional evidence to support the conclusion that moesin-FERM association desorbs the cytoplasmic domain of CLS from the anionic membrane surface.

Binding of moesin-FERM to CLS in POPS liposome is prerequisite for CaM association

In contrast to the facilitation of moesin-FERM association with CLS by PS lipids, we have reported earlier that CaM binds to CLS in the POPC liposome but not CLS in the POPC/POPS liposome [29]. However, in PMA-stimulated cells, moesin and CaM were observed to form a ternary complex with L-selectin [30]. To elucidate the molecular basis for the interactions among moesin, CaM and CLS, we first explored the possibility of a direct interaction between moesin-FERM and CaM. No significant change in Trp fluorescence emission intensity was observed upon the addition of 10 μM calcium-loaded CaM, which lacks Trp residues, to moesin-FERM (Fig. 6a). Likewise, the titration of up to 10 μM moesin-FERM to 5-((((2-iodoacetyl)amino)ethyl) amino)naphthalene-1-sulfonic acid (IAEDANS)-la-beled CaM (IAEDANS-CaM) produced little change in the IAEDANS fluorescence emission nor its anisotropy (Fig. 6b and c). This is in clear contrast to the significant change in IAEDANS fluorescence that was induced by the association of known CaM ligands as shown in earlier studies [29,41], suggesting that moesin-FERM does not interact directly with CaM.

To probe the association of CaM with the moesin-FERM/CLS/liposome complex, we diluted TMR-CLS reconstituted in the 15% POPS/85% POPC lipo-some into 50 mM Tris, 150 mM NaCl and 0.3 mM $CaCl_2$ (pH 7.4) buffer to a final TMR-CLS concentration of 5 nM. Time-based TMR fluorescence emission at 575 nm was recorded during the addition of moesin-FERM and/or CaM to the TMR-CLS liposome (Fig. 6d and e). Consistent with our earlier finding that CaM does not associate with CLS in anionic membrane [29,42], addition of CaM to TMR-CLS/POPS liposome did not induce a significant change in TMR fluorescence. In comparison, addition of moesin-FERM induced the decrease of TMR fluorescence emission as expected. Following moesin-FERM, addition of calcium-loaded CaM or apo-CaM, but not bovine serum albumin, induced an increase of TMR fluorescence emission (Fig. 6e).

Plotting the TMR fluorescence change as a function of CaM concentration produced an apparent K_d around 1 μM that was independent of calcium ion (Fig. 6e and Table 1), which is similar to that of CaM association with CLS/POPC liposome [29,42]. Overall, our results indicate that association of moesin-FERM with CLS/POPC/POPS desorbs the cytoplas-mic domain of CLS from the anionic membrane surface and, consequently, makes it accessible to CaM association.

Discussion

In the present study, we have characterized the association of moesin-FERM with CLS, the protein fragment that contains both transmembrane and cytoplasmic domains of L-selectin, in lipid membrane conditions. While the association of moesin-FERM to CLS in a zwitterionic membrane environment is similar to that of moesin-FERM to the water-soluble L-selectin cytoplasmic peptide in the aqueous environment, it is strengthened in an anionic membrane environment, likely due to the affinity of moesin-FERM to anionic lipids. More importantly, we have found, for the first time, that the association of moesin-FERM leads to the dissociation of the cytoplasmic domain of L-selectin from the membrane surface, thus making it accessible to other intracel-lular proteins such as CaM.

It has been reported that moesin from PMA-stimulated but not unstimulated leukocytes binds immobilized L-selectin cytoplasmic peptide (residues Arg318–Tyr334) [8]. PMA activates protein kinase C as well as Rho-kinases [43–46], which can phos-phorylate residue Thr558 in the C-terminal domain of moesin [47–49]. Phosphorylation of Thr558 destabilizes the self-masked association between N-terminal FERM and C-terminal domains of moesin, thereby enabling the former to bind other proteins as well as lipids (Fig. 7) [18,45,50].

Consistently, we have demonstrated in this study that moesin-FERM, but not full-length moesin, associates with the L-selectin cytoplasmic peptide (Fig. 2). Through fluorescence titration, a K_d of approximately 200 nM was obtained for the association of moesin-FERM (residues 1–346) with ARR18, which is similar in magnitude to a K_d of 40 nM reported earlier for the association of an N-terminal fragment of moesin (residues 1–296) and the immobilized L-selectin cytoplasmic peptide [8]. The difference in K_d values is likely due to the difference in constructs (moesin-FERM versus moesin fragment 1–296; water-soluble ARR18 versus immobilized L-selectin fragment Arg318–Tyr334) and experimental settings (fluorescence titration versus surface plasmon resonance), particularly that the N-terminal fragment 1–296 is much less stable than moesin-FERM (data not shown).

A crystal structure of the radixin FERM domain in complex with inositol trisphosphate revealed a PIP_2-binding site at the junction of F1 and F3 subdomains [51]. In addition, several lysine residues on the surface of the F3 subdomain have been identified to participate in PIP_2 binding [52]. The FERM domain of moesin can also bind to PS, albeit at a weaker affinity [32,33]. Thus, it is conceivable that anionic lipids can recruit moesin-FERM to the membrane and facilitate its association with the cytoplasmic domain of L-selectin by the proximity effect. Indeed, we observed an approximately 5-fold increase in K_d for the association of moesin-FERM with CLS in the anionic membrane (Fig. 4 and Table 1). Although the extent of increase in affinity is smaller than those in other reported cases [53], it is noteworthy that the apparent K_d obtained in this study likely includes the free energy cost required to break the electrostatic interaction between the cytoplasmic domain of L-selectin and the anionic membrane surface. Overall, these results suggest that the membrane bilayer plays a critical role in mediating the association of activated moesin with L-selectin and emphasize the need to study these interactions in the context of appropriate membrane conditions.

CaM was postulated to inhibit shedding of L-selectin by binding to the juxtamembrane region of the L-selectin cytoplasmic domain [6], but the underlying mechanism has remained unclear. The juxtamembrane region of the L-selectin cytoplasmic domain is enriched in basic residues, which adheres electrostatically to the anionic membrane bilayer that mimics the inner leaflet of the plasma membrane [29]. Such adhesion precludes CaM from associating directly with CLS in POPS-containing liposome [29]. In contrast, when CLS is reconstituted in the zwitterionic POPC membrane bilayer, the cytoplas-mic domain is not attached to the membrane surface and it can bind CaM with a modest affinity [29]. Recently, it was shown that CaM forms a ternary complex with L-selectin and moesin in the cell, with both CaM- and moesin-binding sites mapped to the juxtamembrane region of the L-selectin cytoplasmic domain [30]. In this study, we demonstrated that CaM did not bind moesin-FERM directly and that only after moesin-FERM binding did CaM associate with CLS in POPS liposomes (Fig. 6). Therefore, our results suggest, as illustrated in Fig. 7, a sequential binding model for the moesin-FERM/L-selectin/CaM ternary complex: moesin-FERM associates first with L-selectin to induce the separation of the cytoplasmic domain of L-selectin from the anionic membrane surface, which makes the latter accessible to subsequent CaM association. It is also possible that the moesin-FERM association can enable association of another potential shedding regulator to the L-selectin cytoplasmic domain, provided that it can out-compete CaM.

It is noteworthy that CaM association in the ternary complex in the POPS liposome did not require calcium ion (Fig. 6), which is consistent with the earlier report that ethylene glycol bis(β-aminoethyl ether) N,N'-tetraacetic acid had little effect on the association of CaM with moesin FERM domain and L-selectin cytoplasmic peptide in solution [30]. The lack of dependence on calcium ion explains the modest affinity as well as the extended conformation CaM adopts for the moesin-FERM/CLS complex in the liposome [42]. Our

earlier analysis showed that CaM association with ARR18 in solution, which exhibited a similar calcium-independent binding affinity (Table 1), is dynamic and utilizes both of its lobes [29]. Since calcium-loaded CaM is capable of binding many other intracellular proteins with a much higher affinity, it is conceivable that, upon calcium influx in the cell, many intracellular CaM ligands will out-compete moesin-FERM/L-selectin for CaM binding and thereby induce CaM dissociation from L-selectin. This could explain the dissociation of CaM from L-selectin upon cell activation and, relatedly, the inhibitory role of CaM in the regulation of L-selectin shedding [6]. Since moesin-FERM association with the L-selectin cytoplasmic domain is still required for making the latter accessible for binding with another potential shedding activator, moesin-FERM binding is therefore facilitative to L-selectin shedding [8,13]. Many membrane receptors contain in their cyto-plasmic domains a juxtamembrane region that is enriched in basic residues. This positively charged region helps to control the transmembrane topology of the host protein [54]. It has been shown in a number of receptors that this juxtamembrane region adheres to the cytoplasmic surface of the plasma membrane that is enriched in anionic lipids [55–57]. The desorption of this region from the membrane surface, as a result of cell activation, change in the lipid composition or change in sequence modification, is often associated with the regulation of receptor activity. In this study, we have demonstrated in model phospholipid membranes that the FERM domain of moesin binds the cytoplasmic domain of L-selectin and desorbs it from the anionic membrane surface. The FERM domain-induced desorption of the basic-rich cytoplasmic domain from the anionic membrane surface may be a common phenomenon in stimulated cells.

Materials and Methods

Materials

In preparation of L-selectin fragments and fluorescently labeled derivatives, wild-type CaM and its mutants, the FERM domain of human moesin (residues 1–346) has been described previously [29,31,42]. Restriction enzymes were from New England Biolabs (Ipswich, MA). Thrombin and glutathione 4B Sepharose beads were purchased from GE Healthcare (Pittsburgh, PA). TMR and IAEDANS fluorophores were purchased from Anaspec (Fremont, CA) and Invitrogen (Carlsbad, CA), respectively. All synthetic phospholipids were purchased from Avanti Polar Lipids (Alabaster, AL).

Expression and purification of full-length moesin

The DNA fragment encoding human moesin (residues 1–577) was amplified using primers 5′-GCATGAATTC-CATGCCCAAAACGATC-3′ and 5′-GCATCTCGAGTGA-CATAGACTC-3′ and subcloned as an EcoRI/XhoI fragment into the pHex vector to produce a glutathione S-transferase (GST)-moesin fusion protein [58]. Expression, purification and cleavage of the GST-moesin protein was carried out following the protocol that had been established for the production of moesin FERM domain [42]. After thrombin cleavage of the GST-moesin fusion protein, the mixture was loaded onto a re-equilibrated glutathione Sepharose 4B column to separate moesin from GST-containing fragments. Moesin was further purified by gel-filtration chromatography in buffer A [50 mM Tris–HCl, 150 mM NaCl and 1 mM DTT (pH 7.4)]. Its purity was confirmed by SDS-PAGE, and its concentration was measured using an extinction coefficient of 58,800 M^{-1} cm^{-1} at 280 nm. The concentrated protein stock was stored at −80 °C before use.

Association of moesin fragments with water-soluble L-selectin fragments

ARR18 and TMR-ARR18 peptides were prepared as described previously [29]. To titrate full-length moesin or moesin-FERM into TMR-ARR18, we diluted the stock solution of TMR-ARR18 into buffer A to achieve the final concentration of approximately 5 nM. The

moesin sample was prepared by diluting the moesin concentrated stock into TMR-ARR18-containing buffer A so that the TMR-ARR18 concentration was kept constant during the titration. All the solutions were filtered with 0.2-um filter prior to the experiments. The steady-state TMR emission fluorescence was acquired on a PTI QuantaMaster spectrometer (Photon Technology International, Birmingham, NJ) using a 3-ml cuvette. The excitation and emission wavelength was 542 nm and 575 nm, respectively. The slit widths for excitation and emission were adjusted to minimize photo bleaching of the sample and to achieve sufficient fluorescent signal intensity. Titration of unlabeled ARR18 into moesin-FERM (or full-length moesin) followed similar steps. Emission fluorescence of Trp residues in moesin was used as the indicator for the titration, with the excitation and emission wavelengths set to 295 nm and 333 nm, respectively.

When applicable, the plot of fluorescence intensity as a function of ligand concentration was fitted with the hyperbolic function

$$F = F_f + \frac{[\mathrm{ligand_f}](F_b - F_f)}{K_d} + [\mathrm{ligand_f}]$$

where F is the observed fluorescence, F_f is the fluorescence of unbound substrate, F_b is the fluorescence of the ligand-substrate complex, $[\mathrm{ligand_f}]$ is the concentration of the free ligand and K_d is the dissociation constant.

Reconstitution of TMR-CLS in liposomes

CLS containing the S329C mutation has been described previously [31]. The A317C mutation was introduced to the CLS gene fragment using the primer 5′-CATTTGGCTGTGTAGGAGATTAAAAAAAGGC and its complementary primer. Conjugation of TMR to CLS was carried out as described previously [31]. Reconstitution of TMR-CLS in liposomes consisting of desired phospho-lipids followed the published procedure that used the mini-extruder and the 400-nm pore-sized filter [29]. The molar ratio of TMR-CLS to lipid was maintained at 1:1000 throughout this study. The concentration of TMR-CLS in a liposome sample was determined by diluting 20 μl aliquot into 480 μl of the same aqueous buffer containing 10% SDS and then measuring the TMR emission fluorescence intensity (with excitation and emission wavelengths at 542 and 575 nm, respectively). The fluorescence intensity was used to determine the concentration of TMR-CLS by comparing to a standard curve as described previously [29].

Association of moesin fragments with TMR-CLS in phospholipid liposomes

Both TMR-CLS(317) and TMR-CLS liposomes were prepared in buffer A. Titration of moesin to TMR-conjugated CLS (approximately 5 nM final concentration) reconstituted in the liposome was monitored by the change in TMR fluorescence emission at 20 °C using a 1-ml cuvette. The excitation wavelength was set to 542 nm. Each spectrum was the average of three scans. Empty liposomes of the same lipid composition but without CLS were used for correction of background reading. Dissociation constants were obtained by fitting the titration curves to the hyperbolic equation as described above.

Fluorescence anisotropy measurement

Fluorescence anisotropy experiments were performed on the same PTI fluorimeter with polarizers installed. For each measurement, desired amount of moesin-FERM in 50 mM Tris–HCl (pH 7.4) buffer that contained 150 mM NaCl and 0.3 mM CaCl$_2$ was titrated into 125 nM IAEDANS-CaM in the same buffer. The excitation wavelength was set to 340 nm,

and the fluorescence emission at 475 nm was measured. Fluorescence anisotropy (A) of IAEDANS-CaM at any given concentration of moesin-FERM was calculated as previously described [59] and averaged from three independent measurements.

Time-based TMR fluorescence measurement

TMR-CLS/15% POPS/85% POPC liposome stock was diluted into 2 ml of 50 mM Tris–HCl (pH 7.4) buffer that contained 150 mM NaCl and 0.3 mM $CaCl_2$ to achieve a final concentration of approximately 5 nM. Both moesin-FERM and CaM in the same buffer were added at various time points into this solution. The TMR emission fluorescence was recorded over time with excitation and emission wavelengths set to 542 nm and 575 nm, respectively. A stirring bar was put in the cuvette to ensure thorough mixing of the samples. The recording was paused when titrating samples into the cuvette. The scanning speed was once per second.

Acknowledgments

References

1. Arribas J, Borroto A. Protein ectodomain shedding. Chem Rev. 2002; 102:4627–38. [PubMed: 12475204]

2. Weber S, Saftig P. Ectodomain shedding and ADAMs in development. Development. 2012; 139:3693–709. [PubMed: 22991436]

3. Dreymueller D, Pruessmeyer J, Groth E, Ludwig A. The role of ADAM-mediated shedding in vascular biology. Eur J Cell Biol. 2012; 91:472–85. [PubMed: 22138087]

4. Higashiyama S, Nanba D, Nakayama H, Inoue H, Fukuda S. Ectodomain shedding and remnant peptide signalling of EGFRs and their ligands. J Biochem. 2011; 150:15–22. [PubMed: 21610047]

5. Hartmann M, Herrlich A, Herrlich P. Who decides when to cleave an ectodomain? Trends Biochem Sci. 2013; 38:111–20. [PubMed: 23298902]

6. Kahn J, Walcheck B, Migaki GI, Jutila MA, Kishimoto TK. Calmodulin regulates l-selectin adhesion molecule expression and function through a protease-dependent mechanism. Cell. 1998; 92:809–18. [PubMed: 9529256]

7. Rosen SD. Ligands for l-selectin: homing, inflammation, and beyond. Annu Rev Immunol. 2004; 22:129–56. [PubMed: 15032576]

8. Ivetic A, Deka J, Ridley A, Ager A. The cytoplasmic tail of l-selectin interacts with members of the Ezrin-Radixin-Moesin (ERM) family of proteins: cell activation-dependent binding of Moesin but not Ezrin. J Biol Chem. 2002; 277:2321–9. [PubMed: 11706008]

9. Li Y, Brazzell J, Herrera A, Walcheck B. ADAM17 deficiency by mature neutrophils has differential effects on l-selectin shedding. Blood. 2006; 108:2275–9. [PubMed: 16735599]

10. Killock DJ, Ivetic A. The cytoplasmic domains of TNFα-converting enzyme (TACE/ADAM17) and l-selectin are regulated differently by p38 MAPK and PKC to promote ectodomain shedding. Biochem J. 2010; 428:293–304. [PubMed: 20331435]

11. Kahn J, Ingraham RH, Shirley F, Migaki GI, Kishimoto TK. Membrane proximal cleavage of l-selectin: identification of the cleavage site and a 6-kD transmembrane peptide fragment of l-selectin. J Cell Biol. 1994; 125:461–70. [PubMed: 7512970]

12. Matala E, Alexander SR, Kishimoto TK, Walcheck B. The cytoplasmic domain of l-selectin participates in regulating l-selectin endoproteolysis. J Immunol. 2001; 167:1617–23. [PubMed: 11466384]

13. Ivetic A, Florey O, Deka J, Haskard DO, Ager A, Ridley AJ. Mutagenesis of the ezrin-radixin-moesin binding domain of l-selectin tail affects shedding, microvillar positioning, and leukocyte tethering. J Biol Chem. 2004; 279:33263–72. [PubMed: 15178693]

14. Zhao L, Shey M, Farnsworth M, Dailey MO. Regulation of membrane metalloproteolytic cleavage of l-selectin (CD62L) by the epidermal growth factor domain. J Biol Chem. 2001; 276:30631–40. [PubMed: 11375402]

15. Bretscher A. Regulation of cortical structure by the ezrin-radixin-moesin protein family. Curr Opin Cell Biol. 1999; 11:109–16. [PubMed: 10047517]

16. Bretscher A, Chambers D, Nguyen R, Reczek D. ERM-Merlin and EBP50 protein families in plasma membrane organization and function. Annu Rev Cell Dev Biol. 2000; 16:113–43. [PubMed: 11031232]

17. Lankes WT, Furthmayr H. Moesin: a member of the protein 4.1-talin-ezrin family of proteins. Proc Natl Acad Sci USA. 1991; 88:8297–301. [PubMed: 1924289]

18. Pearson MA, Reczek D, Bretscher A, Karplus PA. Structure of the ERM protein moesin reveals the FERM domain fold masked by an extended actin binding tail domain. Cell. 2000; 101:259–70. [PubMed: 10847681]

19. Huang L, Wong TY, Lin RC, Furthmayr H. Replacement of threonine 558, a critical site of phosphorylation of moesin *in vivo*, with aspartate activates F-actin binding of moesin. Regulation by conformational change. J Biol Chem. 1999; 274:12803–10. [PubMed: 10212266]

20. Nakamura F, Huang L, Pestonjamasp K, Luna EJ, Furthmayr H. Regulation of F-actin binding to platelet moesin *in vitro* by both phosphorylation of threonine 558 and polyphosphatidy-linositides. Mol Biol Cell. 1999; 10:2669–85. [PubMed: 10436021]

21. Edwards SD, Keep NH. The 2.7 Å crystal structure of the activated FERM domain of moesin: an analysis of structural changes on activation. Biochemistry. 2001; 40:7061–8. [PubMed: 11401550]

22. Jayasundar JJ, Ju JH, He L, Liu D, Meilleur F, Zhao J, et al. Open conformation of ezrin bound to phosphatidylinositol 4,5-bisphosphate and to F-actin revealed by neutron scattering. J Biol Chem. 2012; 287:37119–33. [PubMed: 22927432]

23. Serrador JM, Alonso-Lebrero JL, del Pozo MA, Furthmayr H, Schwartz-Albiez R, Calvo J, et al. Moesin interacts with the cytoplasmic region of intercellular adhesion molecule-3 and is redistributed to the uropod of T lymphocytes during cell polarization. J Cell Biol. 1997; 138:1409–23. [PubMed: 9298994]

24. Yonemura S, Hirao M, Doi Y, Takahashi N, Kondo T, Tsukita S. Ezrin/radixin/moesin (ERM) proteins bind to a positively charged amino acid cluster in the juxta-membrane cytoplas-mic domain of CD44, CD43, and ICAM-2. J Cell Biol. 1998; 140:885–95. [PubMed: 9472040]

25. Semenova I, Ikeda K, Ivanov P, Rodionov V. The protein kinase A-anchoring protein moesin is bound to pigment granules in melanophores. Traffic. 2009; 10:153–60. [PubMed: 18980611]

26. Shaffer MH, Dupree RS, Zhu P, Saotome I, Schmidt RF, McClatchey AI, et al. Ezrin and moesin function together to promote T cell activation. J Immunol. 2009; 182:1021–32. [PubMed: 19124745]

27. Barreiro O, Yanez-Mo M, Serrador JM, Montoya MC, Vicente-Manzanares M, Tejedor R, et al. Dynamic interaction of VCAM-1 and ICAM-1 with moesin and ezrin in a novel endothelial docking structure for adherent leukocytes. J Cell Biol. 2002; 157:1233–45. [PubMed: 12082081]

28. Ivetic A, Ridley AJ. The telling tail of l-selectin. Biochem Soc Trans. 2004; 32:1118–21. [PubMed: 15506984]

29. Deng W, Srinivasan S, Zheng X, Putkey JA, Li R. Interaction of calmodulin with l-selectin at the membrane interface: implication on the regulation of l-selectin shedding. J Mol Biol. 2011; 411:220–33. [PubMed: 21664913]

30. Killock DJ, Parsons M, Zarrouk M, Ameer-Beg SM, Ridley AJ, Haskard DO, et al. *In vitro* and *in vivo* characterization of molecular interactions between calmodulin, Ezrin/Radixin/-Moesin, and l-selectin. J Biol Chem. 2009; 284:8833–45. [PubMed: 19129194]

31. Srinivasan S, Deng W, Li R. l-selectin transmembrane and cytoplasmic domains are monomeric in membranes. Biochim Biophys Acta. 2011; 1808:1709–15. [PubMed: 21316337]

32. Maniti O, Khalifat N, Goggia K, Dalonneau F, Guerin C, Blanchoin L, et al. Binding of moesin and ezrin to membranes containing phosphatidylinositol (4,5) bisphosphate: a comparative study of the affinity constants and conformational changes. Biochim Biophys Acta. 2012; 1818:2839–49. [PubMed: 22813867]

33. Blin G, Margeat E, Carvalho K, Royer CA, Roy C, Picart C. Quantitative analysis of the binding of ezrin to large unilamellar vesicles containing phosphatidylinositol 4,5 bisphosphate. Biophys J. 2008; 94:1021–33. [PubMed: 17827228]

34. Edman L, Mets U, Rigler R. Conformational transitions monitored for single molecules in solution. Proc Natl Acad Sci USA. 1996; 93:6710–5. [PubMed: 8692883]

35. Eggeling C, Fries JR, Brand L, Gunther R, Seidel CA. Monitoring conformational dynamics of a single molecule by selective fluorescence spectroscopy. Proc Natl Acad Sci USA. 1998; 95:1556–61. [PubMed: 9465054]

36. Gottfried EL. Lipids of human leukocytes: relation to celltype. J Lipid Res. 1967; 8:321–7. [PubMed: 5231291]

37. Hirao M, Sato N, Kondo T, Yonemura S, Monden M, Sasaki T, et al. Regulation mechanism of ERM (ezrin/radixin/moe-sin) protein/plasma membrane association: possible involvement of phosphatidylinositol turnover and Rho-dependent signaling pathway. J Cell Biol. 1996; 135:37–51. [PubMed: 8858161]

38. Castanho M, Prieto M, Acuna AU. The transverse location of the fluorescent probe trans-parinaric acid in lipid bilayers. Biochim Biophys Acta. 1996; 1279:164–8. [PubMed: 8603083]

39. Stromqvist J, Chmyrov A, Johansson S, Andersson A, Maler L, Widengren J. Quenching of triplet state fluorophores for studying diffusion-mediated reactions in lipid membranes. Biophys J. 2010; 99:3821–30. [PubMed: 21112307]

40. Vogel A, Scheidt HA, Huster D. The distribution of lipid attached spin probes in bilayers: application to membrane protein topology. Biophys J. 2003; 85:1691–701. [PubMed: 12944284]

41. Putkey JA, Waxham MN. A peptide model for calmodulin trapping by calcium/calmodulin-dependent protein kinase II. J Biol Chem. 1996; 271:29619–23. [PubMed: 8939892]

42. Deng W, Putkey JA, Li R. Calmodulin adopts an extended conformation when interacting with l-selectin in membranes. PLoS One. 2013; 8:e62861. [PubMed: 23658780]

43. Myers MA, McPhail LC, Snyderman R. Redistribution of protein kinase C activity in human monocytes: correlation with activation of the respiratory burst. J Immunol. 1985; 135:3411–6. [PubMed: 2995492]

44. Smith RJ, Justen JM, Sam LM. Function and stimulus-specific effects of phorbol 12-myristate 13-acetate on human polymorphonuclear neutrophils: autoregulatory role for protein kinase C in signal transduction. Inflammation. 1988; 12:597–611. [PubMed: 2851553]

45. Matsui T, Maeda M, Doi Y, Yonemura S, Amano M, Kaibuchi K, et al. Rho-kinase phosphorylates COOH-terminal threonines of ezrin/radixin/moesin (ERM) proteins and regulates their head-to-tail association. J Cell Biol. 1998; 140:647–57. [PubMed: 9456324]

46. Xiao L, Eto M, Kazanietz MG. ROCK mediates phorbol ester-induced apoptosis in prostate cancer cells via p21Cip1 up-regulation and JNK. J Biol Chem. 2009; 284:29365–75. [PubMed: 19667069]

47. Pietromonaco SF, Simons PC, Altman A, Elias L. Protein kinase C-θ phosphorylation of moesin in the actin-binding sequence. J Biol Chem. 1998; 273:7594–603. [PubMed: 9516463]

48. Jeon S, Kim S, Park JB, Suh PG, Kim YS, Bae CD, et al. RhoA and Rho kinase-dependent phosphorylation of moesin atThr-558 in hippocampal neuronal cells by glutamate. J Biol Chem. 2002; 277:16576–84. [PubMed: 11867620]

49. Nakamura F, Amieva MR, Furthmayr H. Phosphorylation of threonine 558 in the carboxyl-terminal actin-binding domain of moesin by thrombin activation of human platelets. J Biol Chem. 1995; 270:31377–85. [PubMed: 8537411]

50. Ben-Aissa K, Patino-Lopez G, Belkina NV, Maniti O, Rosales T, Hao JJ, et al. Activation of moesin, a protein that links actin cytoskeleton to the plasma membrane, occurs by phos-phatidylinositol 4,5-bisphosphate (PIP2) binding sequentially to two sites and releasing an autoinhibitory linker. J Biol Chem. 2012; 287:16311–23. [PubMed: 22433855]

51. Hamada K, Shimizu T, Matsui T, Tsukita S, Hakoshima T. Structural basis of the membrane-targeting and unmasking mechanisms of the radixin FERM domain. EMBO J. 2000; 19:4449–62. [PubMed: 10970839]

52. Barret C, Roy C, Montcourrier P, Mangeat P, Niggli V. Mutagenesis of the phosphatidylinositol 4,5-bisphosphate (PIP_2) binding site in the NH_2-terminal domain of ezrin correlates with its altered cellular distribution. J Cell Biol. 2000; 151:1067–80. [PubMed: 11086008]

53. Moore DT, Nygren P, Jo H, Boesze-Battaglia K, Bennett JS, DeGrado WF. Affinity of talin-1 for the β3-integrin cytosolic domain is modulated by its phospholipid bilayerenvironment. Proc Natl Acad Sci USA. 2012; 109:793–8. [PubMed: 22210111]

54. von Heijne G. Control of topology and mode of assembly of a polytopic membrane protein by positively charged residues. Nature. 1989; 341:456–8. [PubMed: 2677744]

55. Aivazian D, Stern LJ. Phosphorylation of T cell receptor ζ is regulated by a lipid dependent folding transition. Nat Struct Biol. 2000; 7:1023–6. [PubMed: 11062556]

56. Xu C, Gagnon E, Call ME, Schnell JR, Schwieters CD, Carman CV, et al. Regulation of T cell receptor activation by dynamic membrane binding of the $CD3_\varepsilon$ cytoplasmic tyrosine-based motif. Cell. 2008; 135:702–13. [PubMed: 19013279]

57. Sato T, Pallavi P, Golebiewska U, McLaughlin S, Smith SO. Structure of the membrane reconstituted transmembrane-juxtamembrane peptide EGFR(622-660) and its interaction with Ca^{2+}/calmodulin. Biochemistry. 2006; 45:12704–14. [PubMed: 17042488]

58. Luo SZ, Mo X, Afshar-Kharghan V, Srinivasan S, Lopez JA, Li R. Glycoprotein Ibα forms disulfide bonds with 2 glycoprotein Ibp subunits in the resting platelet. Blood. 2007; 109:603–9. [PubMed: 17008541]

59. Luo SZ, Li R. Specific heteromeric association of four transmembrane peptides derived from platelet glycoprotein Ib-IX complex. J Mol Biol. 2008; 382:448–57. [PubMed: 18674540]

Abbreviations used

|	
CaM	calmodulin
DoxylPC	1-palmitoyl-2-stearoyl-(5-doxyl)-*sn*-glycero-3-phosphocholine
GST	glutathione *S*-transferase
IAEDANS	5-(((((2-iodoacetyl)amino)ethyl) amino)naphthalene-1-sulfonic acid
PMA	phorbol-12-myristate-13-acetate
PIP	$_2$phosphatidylinositol-4, 5-bisphosphate
POPC	1-palmitoyl-2-oleoyl-*sn*-glycero-3-phosphocholine
POPS	1-palmitoyl-2-oleoyl-*sn*-glycero-3-phospho-ʟ-serine
PS	phosphatidylserine
TMR	tetramethylrhodamine-5-maleimide

(a)

(b)
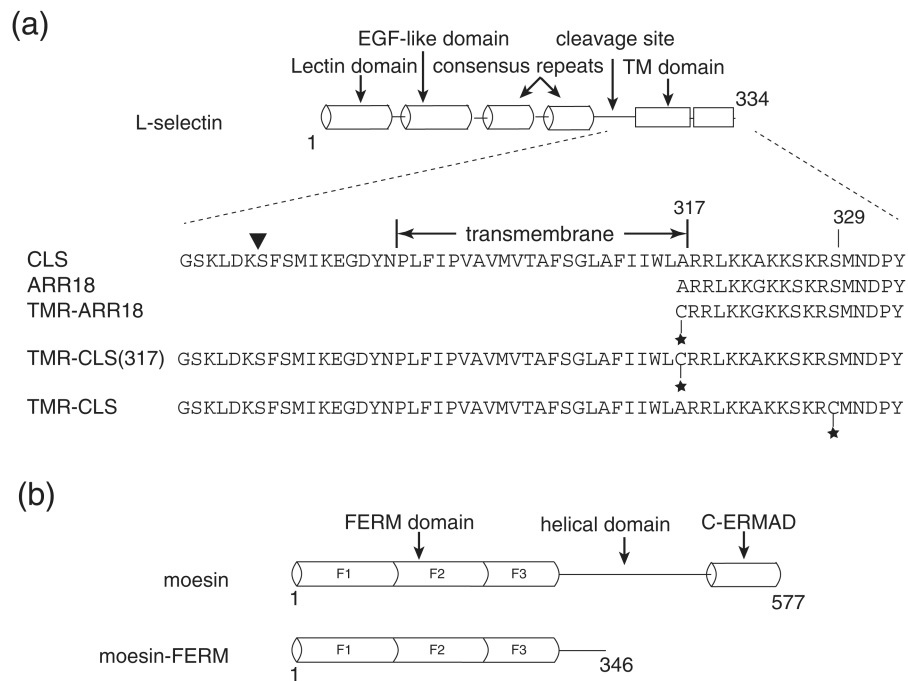
Fig. 1.
Sequence and schematic representation of (a) ʟ-selectin-derived fragments and (b) moesin-derived fragments that are used in this study. Notable domains in both proteins, as well as residue numbers indicating the length of individual fragments, are marked. Sequences of CLS and other ʟ-selectin peptides are shown. The position of TMR conjugation in each fragment is indicated by a star. The shedding cleavage site in ʟ-selectin is indicated by the inverted triangle.
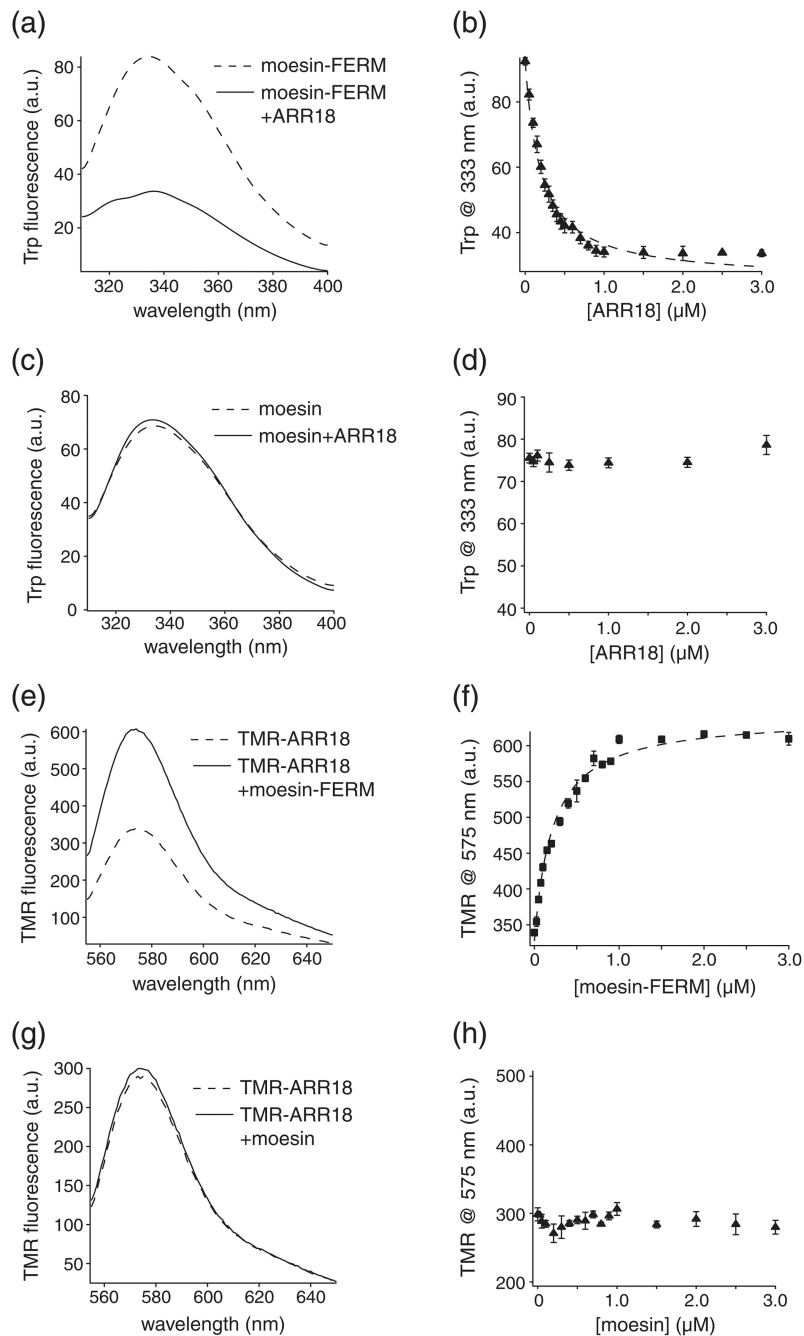
Fig. 2.
ʟ-selectin cytoplasmic peptide binds to moesin-FERM, but not to full-length moesin. (a) Trp fluorescence emission spectra of moesin-FERM in the absence (broken line) and in the presence (continuous line) of 3 μM ARR18 peptide. Moesin FERM domain was dissolved in 50 mM Tris and 150 mM NaCl (pH 7.4) to a final concentration (5 nM). ARR18 peptide in the same solution was added in room temperature. The Trp fluorescence emission spectra were recorded from 310 nm to 400 nm with the excitation wavelength at 295 nm. Each spectrum was the average of three scans and corrected for background signals from the buffer. (b) Binding of ARR18 to moesin-FERM monitored by the change in Trp fluorescence at 333 nm. The broken line indicates the fitted binding curve. (c) Trp

fluorescence emission spectra of full-length moesin in the absence (broken line) and in the presence (continuous line) of 3 μM ARR18. The experimental setting was the same as described in (a). (d) Lack of association of ARR18 with moesin as indicated by the lack of change in Trp fluorescence at 333 nm. (e) TMR fluorescence emission spectra of TMR-ARR18 in the absence (broken line) and in the presence (continuous line) of 3 μM moesin-FERM. The buffer was the same as above. The fluorescence spectra were recorded for 550–650 nm with the excitation wavelength at 542 nm. (f) Binding of moesin-FERM to TMR-ARR18 monitored by the change in TMR fluorescence at 575 nm. The broken line indicates the fitted binding curve. (g) TMR fluorescence emission spectra in the absence (broken line) and in the presence (continuous line) of 3 μM moesin. The experimental setting was the same as in (e). (h) Lack of association of moesin with TMR-ARR18 as indicated by the lack of change in TMR fluorescence at 575 nm.
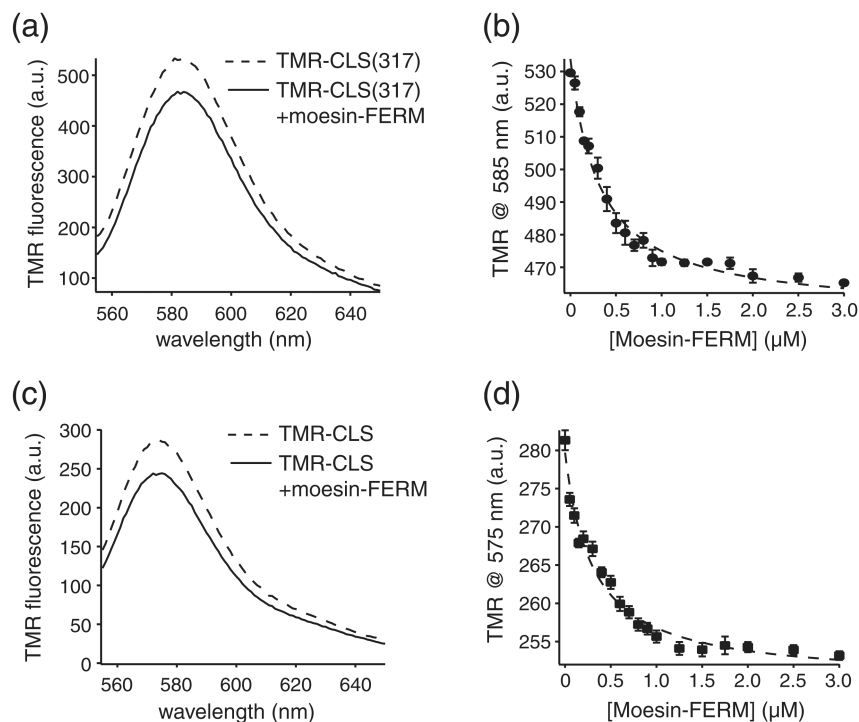
Fig. 3.
Association of moesin-FERM with TMR-CLS(317) and TMR-CLS reconstituted in the POPC liposome, monitored by the change in TMR fluorescence emission. (a and c) TMR fluorescence emission spectra of 5 nM TMR-CLS(317)/POPC or TMR-CLS in the absence (broken line) and in the presence (continuous line) of 3 μM moesin-FERM. The TMR fluorescence emission spectra were recorded for 555–650 nm with the excitation wavelength at 542 nm. Each spectrum was the average of three scans and corrected for background signals from the buffer and the empty liposome. (b and d) Binding of moesin-FERM to TMR-CLS(317)/POPC or TMR-CLS/POPC, monitored by the change in TMR fluorescence at the indicated wavelength. The broken line indicates the fitted binding curve.
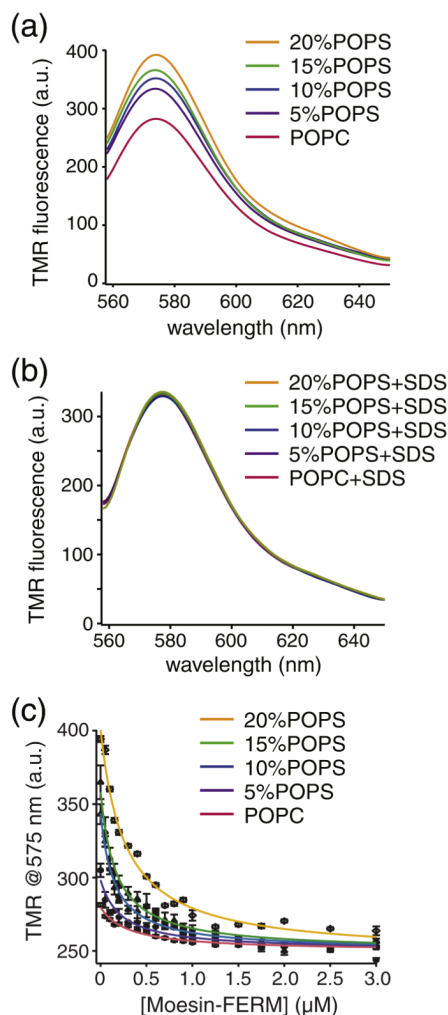
Fig. 4.
POPS facilitates the association of moesin-FERM with TMR-CLS reconstituted in the phospholipid liposome. TMR-CLS/POPC/POPS liposomes, at the pep-tide-to-lipid molar ratio of 1:1000, were prepared and diluted in 50 mM Tris and 150 mM NaCl (pH 7.4) to the final TMR-CLS concentration of 5 nM. Moesin-FERM dissolved in the same buffer containing 5 nM TMR-CLS/POPC/POPS was titrated to the TMR-CLS/POPC/POPS liposome. (a) TMR fluorescence emission spectra of TMR-CLS reconstituted in liposomes of various POPC/POPS composition. Each spectrum is denoted by the percentage of POPS in the liposome. The emission spectra were recorded for 555–650 nm with the excitation wavelength at 542 nm. Each spectrum was the average of three scans and corrected for background signals from the buffer and the empty liposome. (b) TMR fluorescence emission spectra of the same TMR-CLS liposome samples after the addition of 10% SDS to dissolve the liposome. (c) Binding of moesin-FERM to TMR-CLS reconstituted in liposomes of various POPC/POPS composition, monitored by the change in TMR fluorescence at 575 nm. The lines are fitted binding curves to each titration.
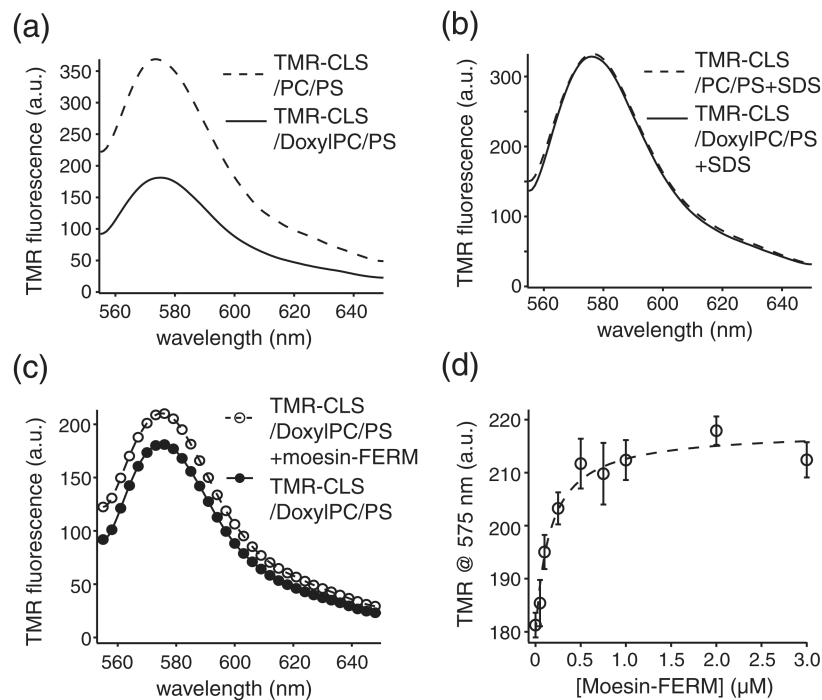
Fig. 5.
Association of moesin-FERM desorbs the cytoplasmic domain of TMR-CLS from the surface of the anionic liposome. (a) TMR fluorescence spectra of TMR-CLS reconstituted in POPC liposomes that also contained 15% POPS (PC/PS) or 10% DoxylPC and 15% POPS (DoxylPC/PS). The TMR-CLS liposome at the same concentration was dissolved in 50 mM Tris–HCl and 150 mM NaCl (pH 7.4). The spectra were recorded for 555–650 nm with the excitation wavelength at 542 nm. Each spectrum was the average of three scans and corrected for background signals from the buffer and the empty liposome. (b) TMR fluorescence emission spectra of the same TMR-CLS liposome samples after the addition of 10% SDS. (c) TMR fluorescence spectra of TMR-CLS/DoxylPC/PS liposome in the absence (●) and in the presence (○) of 3 μM moesin-FERM. (d) Increase of TMR fluorescence emission as a result of titration of moesin-FERM to the TMR-CLS/DoxylPC/PS liposome. The broken line indicates the fitted binding curve.
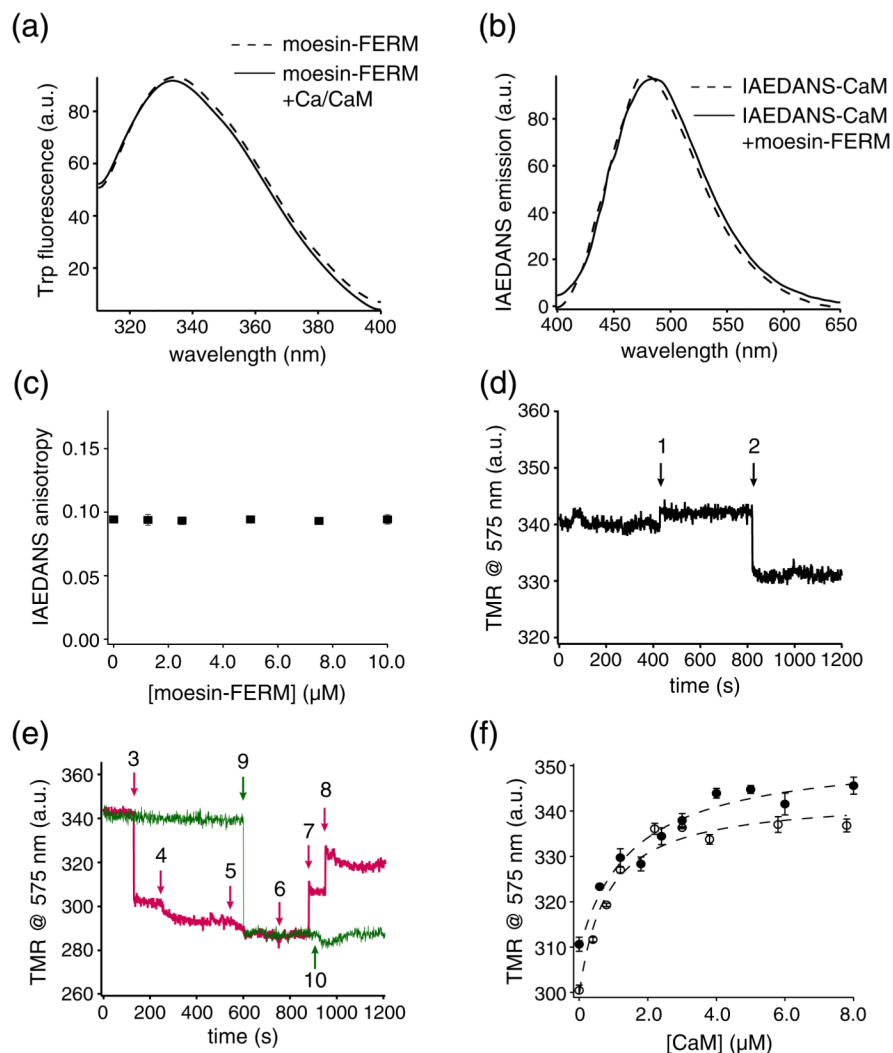
Fig. 6.
CaM interacts only with the moesin-FERM/TMR-CLS complex in the 85% POPC/15% POPS liposome. (a) Trp fluorescence emission spectra of 5 nM moesin-FERM in the absence (broken line) and in the presence (continuous line) of 10 μM CaM in 50 mM Tris–HCl (pH 7.4) buffer containing 150 mM NaCl and 0.3 mM CaCl$_2$. The excitation wavelength was at 295 nm. (b) IAEDANS fluorescence emission spectra of IAEDANS-CaM in the absence (broken line) and in the presence (continuous line) of 10 μM moesin-FERM in the same buffer as above. The excitation wavelength was at 340 nm. Each spectrum was the average of three scans and corrected for background signals from the buffer. (c) Titration plot of fluorescence anisotropy of IAEDANS-CaM *versus* concentration of moesin-FERM added to the mixture. The excitation wavelength was at 340 nm. (d and e) TMR fluorescence emission of TMR-CLS/POPC/POPS liposome at 575 nm was recorded in a time-based fashion with the addition of CaM and/or moesin-FERM at indicated time points. All the additives contained 5 nM TMR-CLS/POPC/POPS. At time point 1, 3 μM Ca/CaM was added to 5 nM TMR-CLS/POPC/POPS liposome in the same buffer shown in (a); at time point 2, 400 nM moesin-FERM was added; at time points 3–6, 100 nM moesin-FERM was added each time; at time points 7 and 8, 1.5 μM CaM was added each time; at time point 9, 400 nM moesin-FERM was added; at time point 10, 1 μM bovine serum

albumin was added. The excitation and emission wavelengths were 542 nm and 575 nm, respectively. (f) Binding of calcium-loaded CaM [Ca/CaM (●)] or apo-CaM (○) to the moesin-FERM/TMR-CLS complex in POPC/POPS liposome, monitored by the change in TMR fluorescence emission at 575 nm. We mixed 400 nM moesin-FERM with 5 nM TMR-CLS/POPC/POPS liposome in the same buffer as above, except that 1 mM ethylenediaminetetraacetic acid instead of 0.3 mM $CaCl_2$ was included for titration of apo-CaM. Broken lines indicate fitted binding curves.
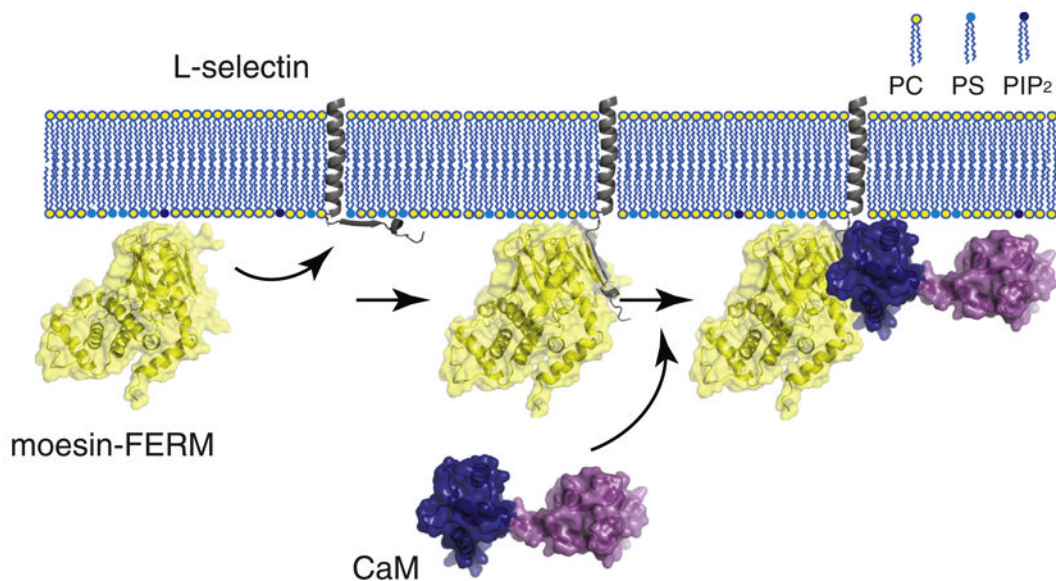
Fig. 7.
A model illustrating formation of the moesin/L-selectin/CaM ternary complex at the membrane interface. The FERM domain of moesin (moesin-FERM) is shown in the yellow-coated ribbon diagram. The transmembrane and cytoplasmic domains of L-selectin are shown in gray, with the former embedded in the membrane bilayer and the latter adhered to the anionic membrane surface. The large extracellular domain of L-selectin is not shown. CaM is shown with its two lobes (shown in dark blue and purple) separated and in an extended conformation. (Left) The FERM domain of moesin is recruited to the membrane due to its association with anionic phospholipids. Meanwhile, the cytoplasmic domain of L-selectin that is enriched in basic residues is associated with anionic membrane surface [29]. (Middle) The FERM domain of moesin binds the cytoplasmic domain of L-selectin and desorbs it from the membrane surface, as shown in this study. CaM alone does not interact with the membrane-adhered cytoplasmic domain of L-selectin [29]. (Right) Only after moesin association does CaM bind the cytoplasmic domain of L-selectin to form the ternary complex, in which CaM takes on an extended conformation [42].

Table 1

Apparent equilibrium dissociation constants measured for various interactions among moesin, L-selectin and CaM fragments

Ligands	L-Selectin fragment	K_d
Moesin-FERM	ARR18	196 ± 15 nM
Moesin-FERM	TMR-ARR18	214 ± 22 nM
Moesin	ARR18	n.d.[a]
Moesin	TMR-ARR18	n.d.[a]
Moesin-FERM	TMR-CLS(317)/POPC[b]	322 ± 43 nM
Moesin-FERM	TMR-CLS/POPC[b]	302 ± 48 nM
Moesin-FERM	TMR-CLS/5% POPS/95% POPC[b]	133 ± 35 nM
Moesin-FERM	TMR-CLS/10% POPS/90% POPC[b]	74 ± 10 nM
Moesin-FERM	TMR-CLS/15% POPS/85% POPC[b]	67 ± 8 nM
Moesin-FERM	TMR-CLS/20% POPS/80% POPC[b]	70 ± 9 nM
Moesin-FERM	TMR-CLS/15% POPS/10% DoxylPC/75% POPC[b]	96 ± 18 nM
Ca/IAEDANS-CaM	ARR18	2.1 ± 0.1 μM[c]
CaM	ARR18	2.5 ± 0.1 μM[c]
Ca/CaM	TMR-CLS/POPC	1.5 ± 0.5 μM[c]
CaM	TMR-CLS/POPC	1.7 ± 0.6 μM[c]
Ca/IAEDANS-CaM	CLS/POPC	2.0 ± 0.4 μM[c]
IAEDANS-CaM	CLS/POPC	3.0 ± 0.4 μM[c]
Ca/CaM	TMR-CLS/15% POPS/85% POPC	n.d.[a,c]
Ca/CaM	moesin-FERM	n.d.[a]
Ca/CaM	CLS/moesin-FERM/15% POPS/85% POPC[b]	1.5 ± 0.3 μM
CaM	CLS/moesin-FERM/15% POPS/85% POPC[b]	0.8 ± 0.2 μM

K_d was obtained by assuming a simple binding reaction as described in Materials and Methods.

[a] Binding was not detected.

[b] The peptide-to-lipid ratio is 1:1000.

[c] This association was examined in an earlier report [29].